Development of a versatile atmospheric N_2O sensor based on quantum cascade laser technology at 4.5 μm

**L. Joly · T. Decarpenterie · N. Dumelié · X. Thomas ·
I. Mappe-Fogaing · D. Mammez · R. Vallon · G. Durry ·
B. Parvitte · M. Carras · X. Marcadet · V. Zéninari**

Abstract We report the development of a field-deployable infrared laser spectrometer using new quantum cascade laser technology at 4.5 μm. The instrument is designed to measure in situ N_2O concentrations at ground level even in bad weather conditions. We provide details of the instrument design and data processing. The long-term stability of the instrument was evaluated using the Allan variance technique. A preliminary evaluation of the instrument performance was realized by in situ measurements of N_2O concentration outside the laboratory.

1 Introduction

The recent increase of atmospheric nitrous oxide, a major anthropogenic contribution to the overall greenhouse effect, is a concern for the atmospheric science community. Since the beginning of the industrial age, the N_2O concentration has increased from ∼250 ppbv to 320 ppbv today. Therefore, it is necessary to acquire a better understanding of the N_2O budget, particularly of the exchanges between the soils and the atmosphere for agronomical studies because agricultural soils contribute substantially to this budget. N_2O

emission occurs due to the use of mineral and organic fertilizers in agricultural activity, through the activity of micro-organisms, and to the expirations of human beings [1]. The production of N_2O by soils primarily occurs through two biological processes: (1) denitrification, the anaerobic microbial respiration using nitrate and nitrite as electrons acceptors [2] and (2) nitrification, the exothermic oxidation of ammonium to nitrite and nitrate [3]. A better understanding of the soil–atmosphere exchange is necessary to control N_2O emissions with new cropping systems. Moreover, N_2O emissions are very variable with time and space [4, 5] and difficult to measure.

Two main methods are available today [6]: (1) the static method, which is based on the measurement of gas concentration within closed chambers that are put at the soil surface during a given period (typically 1 h) and (2) the micrometeorological method, which is based on the measurement of the gas concentration gradient in the atmosphere (Eddy-covariance—EC-method). Needed sensitivity limits in the first case are less than 0.2 ppb in a few seconds and less than 1 ppb in 100 ms in the second one. Drift should be minimal during a period of atmospheric stable condition of about 30 minutes. The measurement frequency should be less than 10 Hz to evaluate the small eddies for the second method. Both methods require gas concentration measurements that are done either in the laboratory after atmospheric sampling or directly in the field. Available gas analyzers limit the possibility to measure the gas concentration on a wide scale and over a long period, while modern atmospheric research on gas exchange between the biosphere and the atmosphere requires sensitive, reliable, and fast response chemical sensors. Therefore, techniques for fast and simultaneously sensitive trace gas measurements based on tunable diode laser absorption spectroscopy have been suc-

L. Joly · T. Decarpenterie · N. Dumelié · X. Thomas ·
I. Mappe-Fogaing · D. Mammez · R. Vallon · G. Durry ·
B. Parvitte · V. Zéninari (✉)
Groupe de Spectrométrie Moléculaire et Atmosphérique, UMR
CNRS 6089, UFR Sciences Exactes et Naturelles, Université de
Reims Champagne-Ardenne, Moulin de la Housse, BP 1039,
51687 Reims Cedex 2, France
e-mail: virginie.zeninari@univ-reims.fr
Fax: +33-326-913147

M. Carras · X. Marcadet
III-V Lab, 1 avenue Augustin Fresnel, 91767 Palaiseau Cedex,
France

Fig. 1 Atmospheric synthetic transmission spectra of N_2O and CO_2 in air with an absorption path length of 76 m at pressure 50 mbar. *Stars* indicate the lines most isolated from others
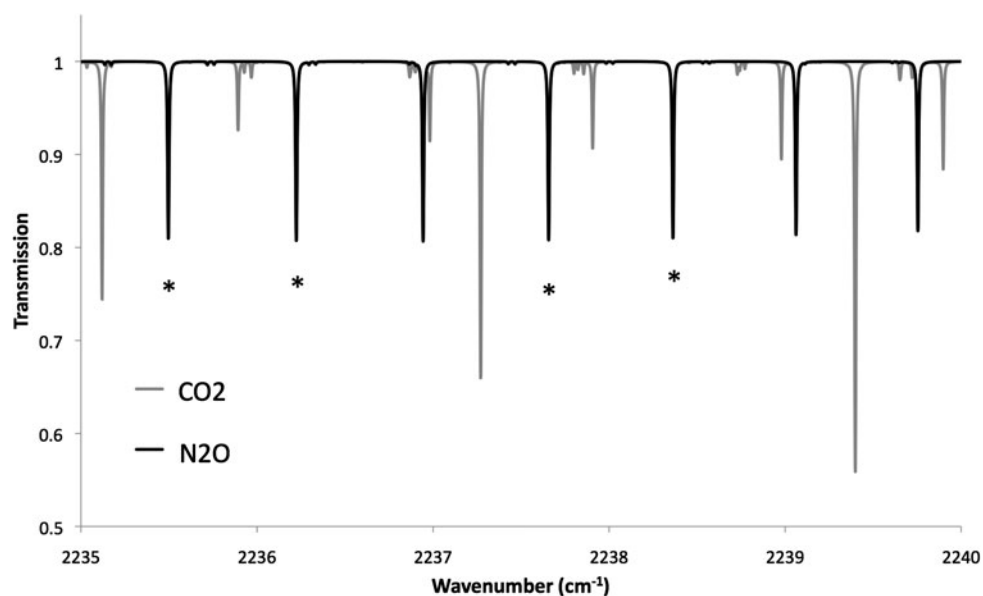
cessfully applied to micrometeorological trace gas flux measurement techniques [7].

Thus laser diode spectrometry is effective to address this issue, by providing accurate nitrous oxide measurements. In particular, a new generation of quantum cascade lasers emitting at room temperature near 4.5 μm are promising tools for the development of highly compact laser field-deployable sensors. The spectral emission properties of these lasers (monochromatic emission, mode-hops free, wavelength tunability over a few cm^{-1}, laser line width of less than 10 MHz, optical output power of from 10 to 100 milliwatts) are very suitable for the determination of gas concentration by infrared absorption spectroscopy. Furthermore, near 4.5 μm, nitrous oxide has strong rotational-vibrational transitions that are well suited for in situ measurement of N_2O in the middle atmosphere.

The recent development of 4.5 μm single frequency quantum cascade lasers by Alcatel-Thales III-V Lab allowed us to develop a field-deployable sensor based on this technology for the in situ determination of atmospheric nitrous oxide [8, 9]. The objective is the development of a compact sensor to monitor N_2O at ground level with a high temporal resolution in order to provide flux measurements in conjunction with wind speed determination. In Sect. 2 we discuss the selection of the laser device and the N_2O rovibronic transitions in the 4.5 μm spectral region, for the purpose of monitoring nitrous oxide. In Sect. 3, the sensor is described and details of the data processing are detailed in the subsequent section. Section 4 presents the laboratory testing of the N_2O sensor. In particular, the long-term stability of the instrument is evaluated using the Allan variance technique. Finally, in Sect. 5, we discuss preliminary in situ measurements achieved with the laser sensor. A set of concentration data over a period of 5 hours is recorded to demonstrate the

capability of the sensor to detect N_2O concentration variations.

2 Laser and spectroscopy

The spectral region of the ν_1 fundamental band around $1285\ cm^{-1}$ (7.8 μm) is a spectral window that has been previously used to detect N_2O simultaneously with methane by semiconductor quantum cascade laser probing in the infrared [10, 11]. In this region the absorption may be of 5% with a pressure of 50 mbar, a pathlength of 100 m and a concentration of 320 ppbv. However, the use of a new generation of quantum cascade lasers with an emission wavelength around $2225\ cm^{-1}$ (4.5 μm) permits one to reach 25% of absorption in the same experimental conditions. Thus the magnitude of the line strengths makes it possible to measure N_2O at ground level with an absorption path length of roughly 100 meters.

However, considerable care must be taken in the choice of the N_2O absorption lines because of potential interference with other atmospheric gases and particularly carbon dioxide. The extreme sensitivity that must be reached needs to minimize interferences with other gases. This issue is illustrated in Fig. 1, which features the absorption spectra of N_2O and CO_2 calculated at atmospheric concentrations for an absorption path length of 76 m at reduced pressure (50 mbar) between $2235\ cm^{-1}$ and $2240\ cm^{-1}$. The appropriate spectroscopic parameters obtained from the HITRAN [12] database are given in Table 1. All these data are quite comparable. Thus, to avoid overlapping with neighboring CO_2 absorption lines, strong and well-isolated N_2O transitions may be selected. A star in Fig. 1 and Table 1 indicates the most convenient lines.

Table 1 Spectroscopic parameters of the main transitions of N$_2$O in the 4.5 μm from HITRAN database. Stars indicate the lines most isolated from others

|	Line position (cm^{-1})	Line intensity at 296 K in natural abundance (10^{-19} cm^{-1}/(molecule cm^{-2}))	Air broadening coefficient (cm^{-1}/atm)	Self broadening coefficient (cm^{-1}/atm)	Energy (cm^{-1})
*	2235.496400	9.999	0.0782	0.1020	87.98450
*	2236.223480	10.04	0.0774	0.1009	100.55250
	2236.943590	9.999	0.0767	0.0998	113.95800
*	2237.656720	9.878	0.0761	0.0988	128.20090
*	2238.362880	9.677	0.0754	0.0978	143.28120
	2239.062060	9.435	0.0749	0.0968	159.19880
	2239.754250	9.153	0.0743	0.0958	175.95360

3 Instrument design

The N$_2$O measurements are performed at high resolution using a direct absorption spectrometer with a new-generation quantum cascade laser. The direct detection technique is straightforward. A photograph of the whole instrument is shown in Fig. 2. The optical part (white box) of the instrument is mounted on a 40×40 cm^2 board. An aspheric ZnSe lens collects the laser beam. The laser beam passes through an absorption cell ($L = 76$ m, $V = 0.5$ L, Herriott-type multiple-reflection cell from Aerodyne). A reflected beam is coupled with a Germanium Fabry–Pérot (FP) interferometer (free spectral range of 0.0161 cm^{-1}) in order to obtain relative frequency calibration. A ZnSe lens focuses both beams on a thermo-electrically cooled infrared sensor PVI-3TE6 from Vigo. The sample gas is brought from atmospheric pressure to #40 mbar to reduce the pressure broadening of the absorption lines, increasing the distinctive nature of the absorbing species spectral signature. The system operates at a gas flow of around 10 L/min. Thus the time of gas sample change inside the cell should be 3 seconds at atmospheric pressure and is there of about 150 ms. A dust filter is set at the inlet of the measurement head to protect the gas system and the mirrors of the cell from pollution. Errors generated by temperature and pressure have been estimated to 1.12 ppb/K and 3.2 ppb/mbar, respectively. Thus the gas pressure and the temperature of the sample must be carefully stabilized.

The room temperature QCL from Alcatel-Thales III-V Lab is mounted onto a copper substrate attached to a thermoelectric cooler [13]. Heat produced by the cooler is evacuated by circulating water through the base of the enclosure. The QCL operates between +10°C and +50°C and the maximum current is 520 mA. A homemade electronic fully integrated rack performs the laser temperature control and the current source. The tunability range of this laser is from 2236 cm^{-1} to 2239 cm^{-1}. The QCL power is #15 mW. The laser emission wavelength is scanned over the molecular transition by applying a current ramp to the QCL. 4096 points are acquired over a standard 7 ms triangular laser scan

Fig. 2 Photograph of the N$_2$O detector set-up. The upper part (*white box*) contains optics and the lower part (*black box*) contains electronics and acquisition part

with a 16-digits resolution and an integrated computer controls the N$_2$O sensor. Usually 10 spectra are co-added. Thus the standard electronic process speed is around 70 ms with a <10 Hz operation. The operating program is developed with C/C++.

Fig. 3 Example of recorded experimental spectrum at 2238.36288 cm^{-1} with calculated spectrum and residual
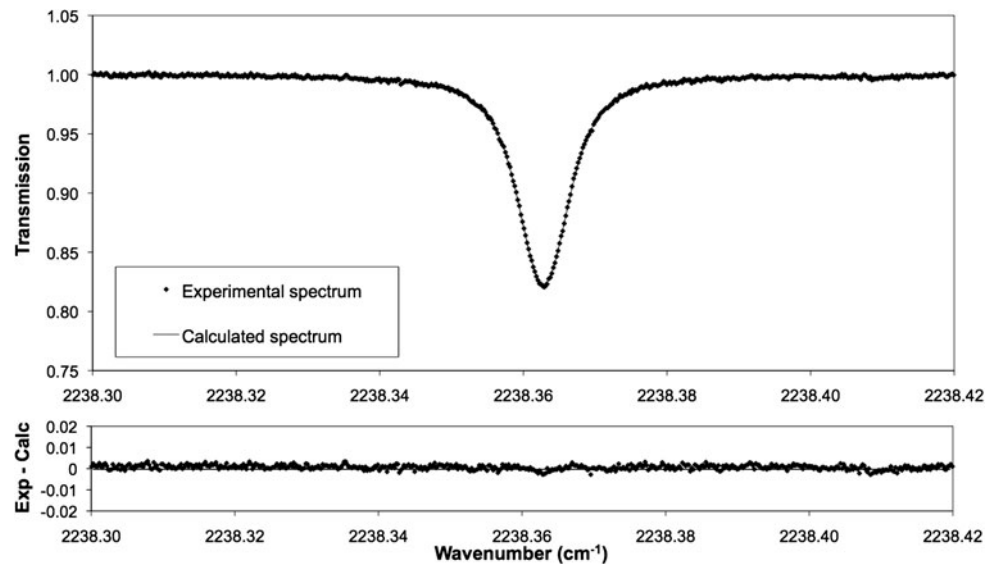
4 Data processing

An example of a recorded spectrum is shown in Fig. 3. The following operations are performed in Python® during data processing:

1. Transmission and Fabry–Pérot (FP) signals are used to perform the wavenumber calibration. The frequency calibration is determined by applying a two-degree polynomial interpolation to the interference fringes in the FP signal. The absolute value of the frequency is known from the position of the main absorption line in the transmission signal.

2. The baseline is determined by applying a third-degree polynomial interpolation over full transmission region on both sides of the absorption line.

3. Once the baseline is determined, the atmospheric transmission can be extracted from the transmission spectrum. The N$_2$O concentration is finally obtained from the transmission by applying a non-linear least square fit to the full molecular line shape using a Voigt model. This type of procedure has been presented elsewhere [14, 15]. Several CO$_2$ lines outside of the laser scanning range are taken into account in the retrieval process to model the atmospheric transmission and to determine the baseline. During the fitting procedure, the N$_2$O mixing ratio and the position of the main N$_2$O line are adjusted.

A result of typical measurement is presented in Fig. 4. Figures 4a, 4b, and 4c provide N$_2$O concentrations, gas pressure and temperature, respectively. These series of measurements were realized on the same air sample. The mean N$_2$O retrieved concentration is 322.3 ppbv. More precisely, a dispersion of 0.87 ppb per 100 ms of measurement is achieved. For a 10 s measurement, the dispersion decreases to 0.176 ppb.

These results are sufficient to develop instruments that are very well adapted for measuring the N$_2$O fluxes on field, determining the factors (soil composition, soil temperature and humidity, quantity of fertilizer...) which favor the N$_2$O emission and showing the annual increase of N$_2$O concentration. For micrometeorological applications [16], the instrument is also capable of sampling high frequency eddies, typically up to 10 Hz.

5 Stability of the instrument and measurements of N$_2$O concentration variation

Stability tests based on the Allan variance method have become a standard procedure for the evaluation of the quality of an instrument. Allan variance distinguishes high frequency random noise from drifts at longer time scales [17–19]. With the Allan variance ($\sigma_A^2(\tau)$), we can specify a noise in a time series due to the relation:

$$\log \sigma_A^2(\tau) = \mu \log \tau \quad \text{for } \tau = \tau_0, 2\tau_0, 4\tau_0, \ldots,$$

where τ_0 is the sampling period in second (s).

- $\mu = -1$ corresponds to white noise,
- $\mu = 0$ to flicker noise,
- $\mu = 1$ to random walk.

An important characteristic of the Allan variance analysis is that it is insensitive to the deterministic content of the analyzed signal (e.g. bias, linear slope, and sine component). We have recorded the time evolution of ambient N$_2$O concentration in a closed circulation. We assumed that the N$_2$O concentration was constant. Thermodynamics parameters were stabilized and pressure and temperature were obtained from the various sensors. Figure 5 shows the corresponding Allan variance of data given in Fig. 4. It depicts a

Fig. 4 Example of measurements in air in close circuit. N$_2$O retrieved concentration, gas pressure and temperature are presented in the same time period
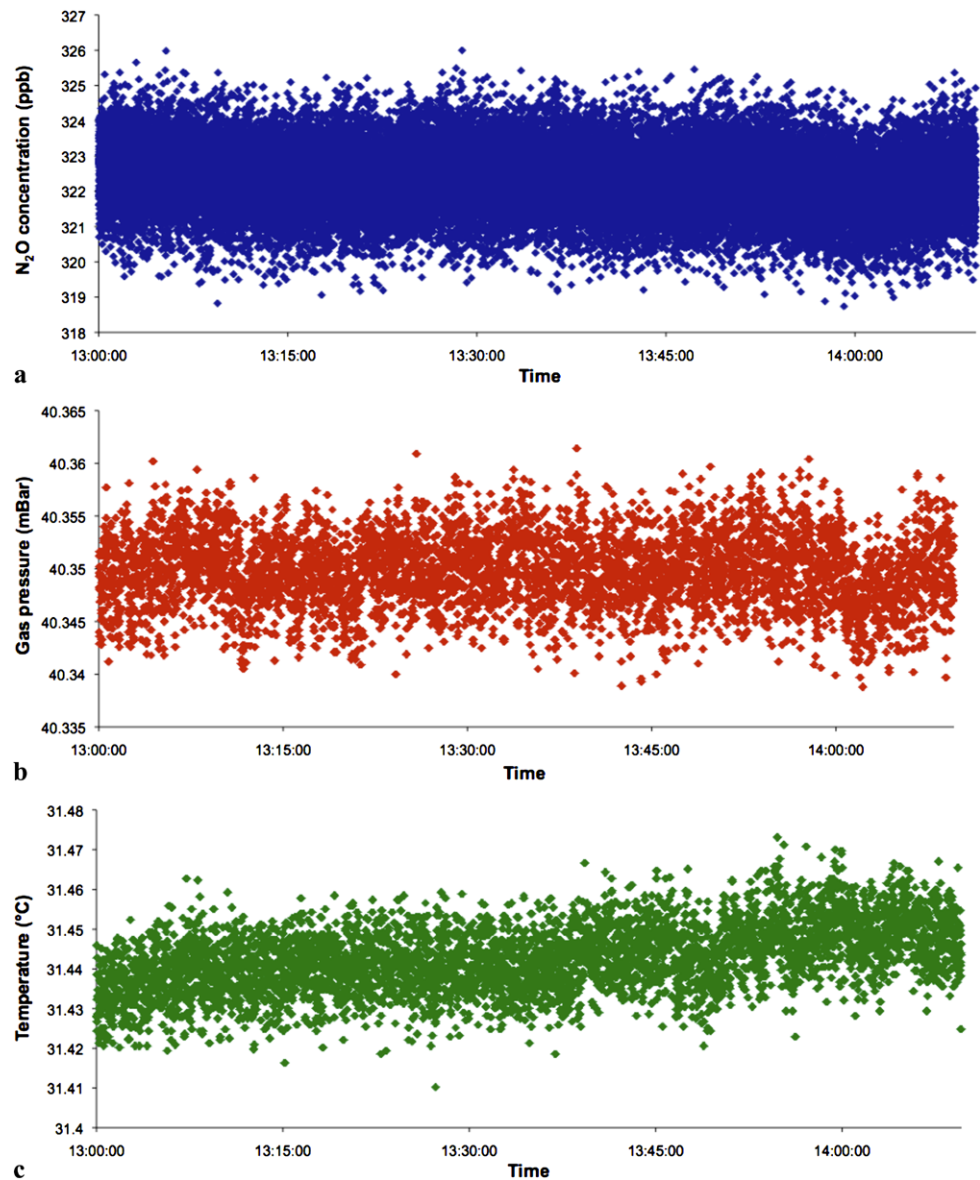
log–log plot of the Allan variance versus the integration time (τ) in seconds. The Allan variance decreases with a slope of -1, and hence only the white noise is dominant up to 909 ms integration time. In most practical cases it is very useful to refer to the particular integration time in the Allan variance plot where the minimum occurs. This minimum describes the turn-over point where the white noise FM with a slope of -1 in the logarithmic plot becomes dominated by additional and undesired drift noise. The variance minimum at $\tau_{Allan} = 909$ ms corresponds to a minimum σ_{Allan} of 42 ppt.

The spectrometer was installed in the laboratory and outside ambient air was pumped via a pipe at about one meter height of the soil. Figure 6 shows the retrieved N$_2$O concentrations during more than ten hours. The mean value during this period is of about 320 ppbv. The weak increasing of the N$_2$O concentration value at the beginning of the recording is maybe related to a temporary weakness of the wind and the fact that the lab is not far from agricultural fields. Another hypothesis is that the observed N$_2$O concentration peak in Fig. 6 is linked to the atmosphere temperature. In fact the emissions of N$_2$O from soils are caused principally by microbial nitrification and denitrification and these processes are controlled by several factors, including temperature [20]. One can also remark in Fig. 6 that no variation was detected during day or night period. A validation of this instrument will be done, during specific field campaigns, by comparison with other instruments such as GC/MS (gas chromatography linked with mass spectrometry). Moreover this spectrometer will be associated to a sonic anemometer and a performing pumping system in order to realize Eddy-correlation measurements. This system will permit a better quantification and understanding of the N$_2$O sources.

Fig. 5 Determination of the Allan variance. *Grey points* correspond to Allan variance measurements and the error is represented in *black*
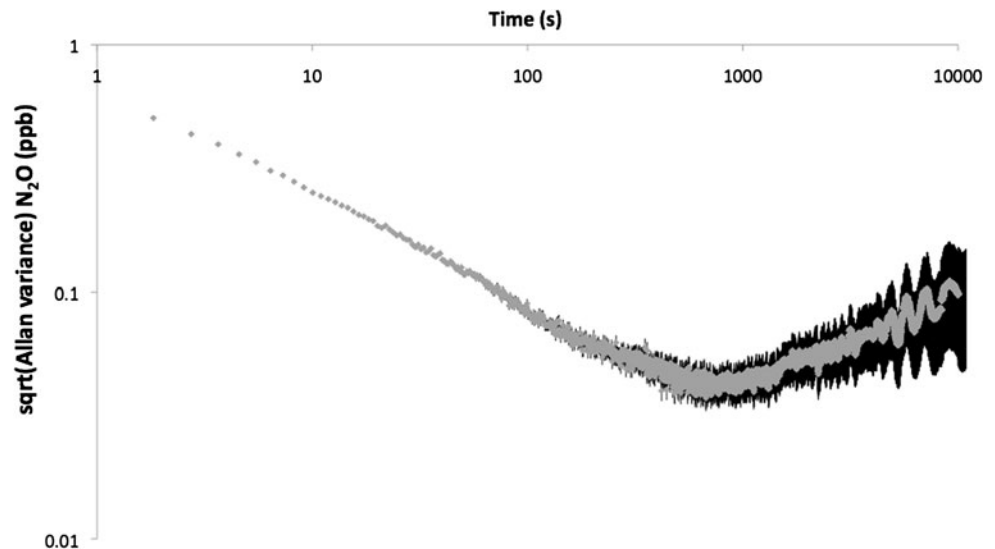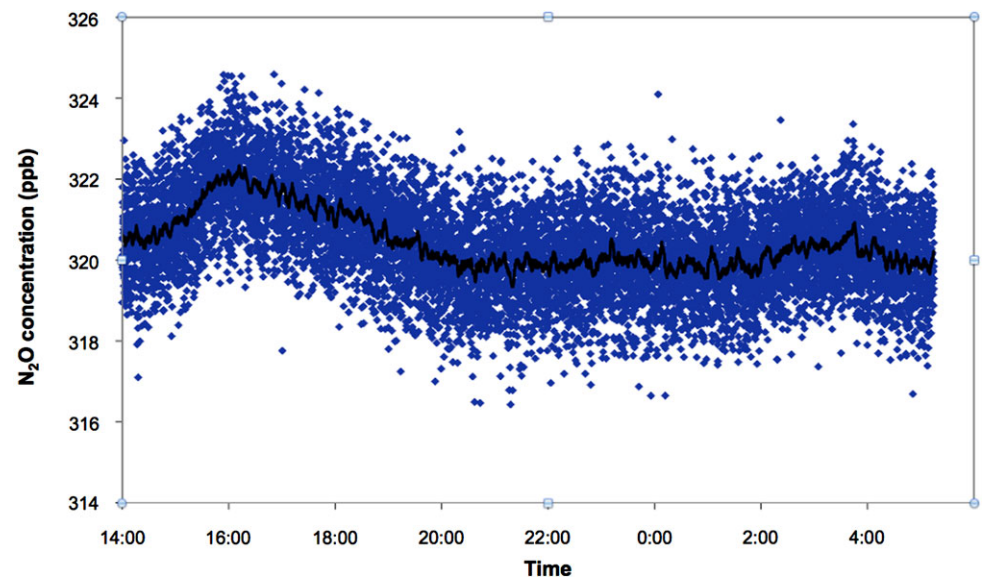

Fig. 6 Preliminary results of atmospheric N_2O measurements. The *black line* is the mean value of *blue experimental points*

6 Conclusions

The development of a field-deployable infrared quantum cascade laser spectrometer has been reported. This instrument is designed to measure N_2O concentrations at ground level. Absorption lines were selected to minimize interferences from neighboring carbon dioxide transitions. However, the possibility to reach a more isolated line should improve again the obtained results. In particular weak CO_2 lines less influence the line @2235.49 cm^{-1} that cannot be reached with our current laser than the currently used line @2238.36 cm^{-1}.

The design of the sensor, details of the data processing technique and the evaluation of the sensors long-term stability with the Allan variance method are reported. A dispersion of 0.87 ppb per 100 ms of measurement is achieved. For a 10 s measurement, the dispersion decreases to 0.176 ppb.

With a longer integration, detection limit improves again. These results demonstrate that the developed instrument is well adapted for Eddy-correlation measurements (<1 ppb in <100 ms needed) and also for the long-term monitoring of N_2O concentrations (<0.2 ppb in 10 s needed). To evaluate the performance of our quantum cascade laser based sensor, atmospheric nitrous oxide was measured for a period of more than ten hours with the instrument. The next step will consist in the set-up industrialization and the participation to in situ campaigns.

References

1. T. Mitsui, M. Miyamura, A. Matsunami, K. Kitagawa, N. Arai, Clin. Chem. **43**, 1993 (1997)
2. R. Knowles, Microbiol. Rev. **46**, 43 (1982)
3. J.I. Prosser, *Nitrification* (IRL Press, Oxford, 1986)
4. J.M. Duxbury, D.R. Bouldin, R.E. Terry, R.L. Tate III, Nature **298**, 462 (1982)
5. H. Flessa, R. Ruser, R. Schilling, N. Loftfield, J.C. Munch, E.A. Kaiser, F. Beese, Geoderma **105**, 307 (2002)
6. A.F. Bouwman, Nutr. Cycl. Agroecosyst. **46**, 53 (1996)
7. M.S. Zahniser, D.D. Nelson, J.B. McManus, P.L. Kebabian, Philos. Trans. R. Soc. Lond., Ser. A **351**, 371 (1995)
8. M. Carras, M. Garcia, X. Marcadet, O. Parillaud, A. De Rossi, S. Bansropun, Appl. Phys. Lett. **93**, 011109 (2008)
9. M. Carras, G. Maisons, B. Simozrag, M. Garcia, O. Parillaud, J. Massies, X. Marcadet, Appl. Phys. Lett. **96**, 161105 (2010)
10. A. Grossel, V. Zéninari, B. Parvitte, L. Joly, D. Courtois, Appl. Phys. B **88**, 483 (2007)
11. L. Joly, C. Robert, B. Parvitte, V. Catoire, G. Durry, G. Richard, B. Nicoullaud, V. Zéninari, Appl. Opt. **47**, 1206 (2008)
12. L.S. Rothman, I.E. Gordon, A. Barbe, D. ChrisBenner, P.F. Bernath, M. Birk, V. Boudon, L.R. Brown et al., J. Quant. Spectrosc. Radiat. Transf. **110**, 533 (2009)
13. www.3-5lab.fr
14. V. Zéninari, B. Parvitte, L. Joly, T. Le Barbu, N. Amarouche, G. Durry, Appl. Phys. B **85**, 265 (2006)
15. M. Mulier, V. Zéninari, L. Joly, T. Decarpenterie, B. Parvitte, P. Jeandet, G. Liger-Belair, Appl. Phys. B **94**, 725 (2009)
16. J. Moncrieff, R. Valentini, S. Greco, G. Seufert, P. Ciccioli, J. Exp. Bot. **48**, 1133 (1997)
17. D.W. Allan, IEEE Trans. Ultrason. Ferroelectr. Freq. Control **34**, 647 (1987)
18. D.W. Allan, Proc. IEEE **54**, 221 (1966)
19. E.S. Ferre-Pikal, J.R. Vig, J.C. Camparo, L.S. Cutler, L. Maleki, W.J. Riley, S.R. Stein, C. Thomas, F.L. Walls, J.D. White, in *Proc. IEEE Int. Freq. Control Symp.* (1997), p. 338
20. D.R. Keeney, I.R. Fillery, G.P. Marx, Soil Sci. Soc. Am. J. **43**, 1124 (1979)